


Contents

Table of Contents	i
List of Figures	i
List of Tables	iii
1 Coupling NDs	1
1.1 Additional Experimental Methods	1
1.1.1 Nanomanipulator	2
1.1.2 Determination of The Position of Nanodiamonds	4
1.1.3 The Pick-And-Place Process	4
1.2 VCSELs	5
1.2.1 Vertical-Cavity Surface Emitting Laser Structure	6
1.2.2 SiV center in a Vertical-Cavity Surface Emitting Laser	6
1.3 Antennas	8
1.3.1 Nanodiamond With Multiple SiV centers Coupled to Antenna	8
1.3.2 Nanodiamond With Single SiV center Coupled to Antenna	8
Bibliography	15

List of Figures

1.1	(a) Sketch of the pick-and-place process exploiting a nanomanipulator. (b) Image of the nanomanipulator mounted in the FIB. The arrows indicate the degrees of freedom of motion of the nanomanipulator. The custom made workbench is situated in the middle of the picture. On top of it, there is a 1 cm^2 substrate with coated nanodiamonds, the nanomanipulator tip pointing to the middle of it. Behind it, there is the target vertical-cavity surface emitting laser. Perpendicular to the workbench, the objective of the electron microscope can be seen. The pointier cone perpendicular to the image top image edge is the objective of the focussed ion beam.	3
1.2	(a) Overview of a field of cross markers. The field spans $0.5 \times 0.5\text{ mm}$ (b) White light scan of an area with a cross marker in all four corners.	3
1.3	5
1.4	(a) Sketch of the VCSEL showing the different layers. ask how to cite (b) Image of the VCSEL. The circle with the black dots is the hole in the p-contact (diameter D_S , the smaller darker area in the middle is the laser output area (diameter D_A)	6
1.5	(a) Emission spectrum of the used VCSEL at two different currents. (b) Optical output power and voltage of the same VCSEL in dependence of input current. []	7
1.6	(a) SEM image of an array of VCSELs. The three wires are the anodes, which are connected to the top layer (p-contact) of the VCSEL. Therefore, three of the VCSEL structures can be operated. (b) Detail SEM image of the top of the exploited VCSEL Bm4. The circular middle part is the hole in the p-contact through which the top DBR is visible. The active diameter is smaller than that and not visible in the SEM.	7
1.7	(a) Scan of the VCSEL Bm4 with coupled nanodiamond under excitation with the laser from the confocal setup. The big visible ring is the edge of the circular hole in the p-contact. The bright spot in the upper left corner corresponds to the transferred nanodiamond containing an SiV center. (b) Scan of the VCSEL Bm2 without nanodiamond under excitation with the laser from the confocal setup. The circular hole in the p-contact exhibits a constant countrate.	8
1.8	<caption>	9
1.9	<caption>	9
1.10	Reflectivity of the DBR of the VCSEL, and spectra of the VCSEL measured in the confocal setup.	9
1.12	<caption>	10

1.13 <caption>	11
1.14	11
1.15 <caption>	11
1.16 <caption>	12
1.17 <caption>	12
1.18 <caption>	12
1.19 <caption>	13
1.20 <caption>	13
1.21 <caption>	13
1.22 <caption>	14

List of Tables

Chapter 1

Coupling Nanodiamonds to Photonic Structures

In the last chapter, we saw that the spectroscopic properties of SiV centers vary strongly among individual nanodiamonds. Nanodiamonds are further implemented in photonic structures for the application in metrology as well as in quantum cryptography or quantum computing. Therefore, it is important to have a good knowledge of the spectroscopic properties of the individual SiV center. A preselection of nanodiamonds including an SiV center with optimal properties is performed. These properties contain both spectroscopic parameters as well as technical parameters for the pick-and-place process. Spectroscopic parameters contain narrow linewidth, high countrates and single photon emission, the technical parameters include a size of the nanodiamonds hosting the SiV center bigger than 70 nm and how isolated they lie on the substrate surface. The selected nanodiamond is then transferred to a target structure. In the scope of this thesis, nanodiamonds including SiV centers were coupled to two different kinds of structures:

- Vertical-Cavity Surface Emitting Lasers: The aim is to create a hybrid-integrated single photon source, where an electric current is employed to create single photons. The diamond containing an SiV center is placed directly on the beam output. Hence the SiV center is directly pumped by the laser beam. This system is interesting for metrological applications, as it is the major building block for a portable device ready to calibrate single photon detectors.
- Plasmonic Nanoantennas: The aim is to enhance photoluminescence intensity. As described in previous chapters, not only ZPL position and linewidth, but also the photoluminescence intensity varies strongly among individual SiV centers. However, in metrology a photon flux rate high enough to be measured by a low optical flux detector is needed [1]. This increase in intensity is achieved by coupling the SiV centers in nanodiamonds to plasmonic antennas.

think
of other
word

1.1 Additional Experimental Methods

To couple nanodiamonds to photonic structures, we pursued several different methods:

1. Directly spin-coat the structures with a nanodiamond solution and consecutively look for a structure containing a nanodiamonds with an SiV center exhibiting the desired spectroscopic properties. This method was tried with the antenna structures, as there are many antenna structures on one substrate (see Figure 1.12a), therefore there is a chance that a suited nanodiamond is incidentally ends up at the right spot. However, it is not suitable for the VCSELs, first because of the morphology of the VCSELs and secondly, because there is a very limited number of VCSELs on one substrate.
2. Use an iridium substrate covered with nanodiamonds containing SiV centers, look for a suited nanodiamond and transfer it with a pick-and-place technique using a nanomanipulator. The nanomanipulator is essentially a thin tip in a scanning electron microscopy. The iridium substrate is preprocessed with markers, to record the position of the preselected nanodiamond. The huge advantage is that the very best suited nanodiamond can be preselected. However, disadvantages of this process include the electron radiation during the pick-and-place process, which might affect SiV center fluorescence light and the further restriction that the nanodiamonds must be big enough to be picked up with the nanomanipulator.
3. Similar to method 2, however the transfer is performed with an atomic force microscope. While this method has the advantage that the nanodiamonds are not irradiated with electrons, the disadvantage is that it is not possible to observe the picking process in real time. The area of the preselected nanodiamond has to be scanned after every pick-up try, which is very time consuming and therefore was not further pursued after some trials.

In the following paragraphs, the pick-and-place technique of method 2 is described in more detail. It is the coupling method most extensively deployed in the scope of this thesis and requires a range of experimental setups. The pick-and-place process was carried out with major help from C. Pauly, group of xxx Mücklich, Saarland University. The nanomanipulator setup was provided by the same group.

1.1.1 Nanomanipulator

In general, nanomanipulator is a tip mounted inside an SEM, allowing manipulation and visualization of the manipulation process at the same time. The one used for our experiments was built by the company Kleindiek (model MM3A-EM) and has a changeable tungsten tip (see Figure 1.1b). It is mounted inside a Thermo Scientific™ Helios NanoLab™ DualBeam™ microscope, which combines a focussed ion beam and an electron microscope. The bent nanomanipulator tip has 3 degrees of freedom: up/down and left/right both in an arc up to 240° and 12 mm in/out (see arrows in Figure 1.1b). Before nanomanipulation the tip was "sharpened" with the focussed ion beam by etching away tungsten with gallium ions. This sharpening was performed to meet the size criteria necessary to pick up the nanodiamonds. In Figure 1.3a the sharpened tip is shown (the radius of curvature amounts to 100 nm). The small tip sticking out of the bigger cone is the sharp tip used for pick-and-place.

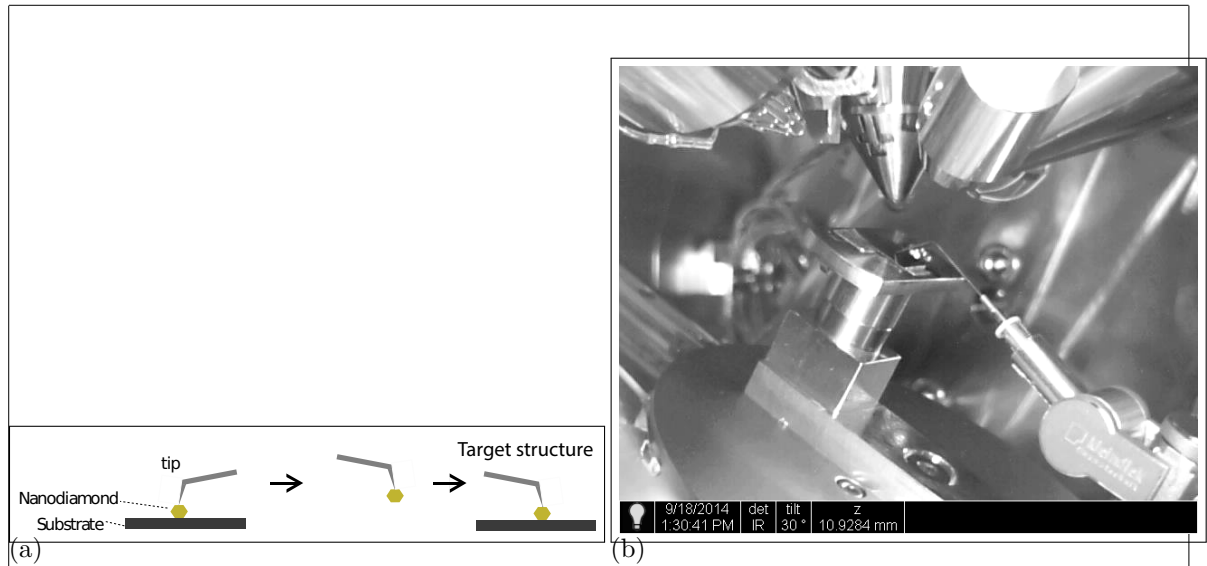


Figure 1.1: (a) Sketch of the pick-and-place process exploiting a nanomanipulator. (b) Image of the nanomanipulator mounted in the FIB. The arrows indicate the degrees of freedom of motion of the nanomanipulator. The custom made workbench is situated in the middle of the picture. On top of it, there is a 1 cm^2 substrate with coated nanodiamonds, the nanomanipulator tip pointing to the middle of it. Behind it, there is the target vertical-cavity surface emitting laser. Perpendicular to the workbench, the objective of the electron microscope can be seen. The pointier cone perpendicular to the image top image edge is the objective of the focussed ion beam.

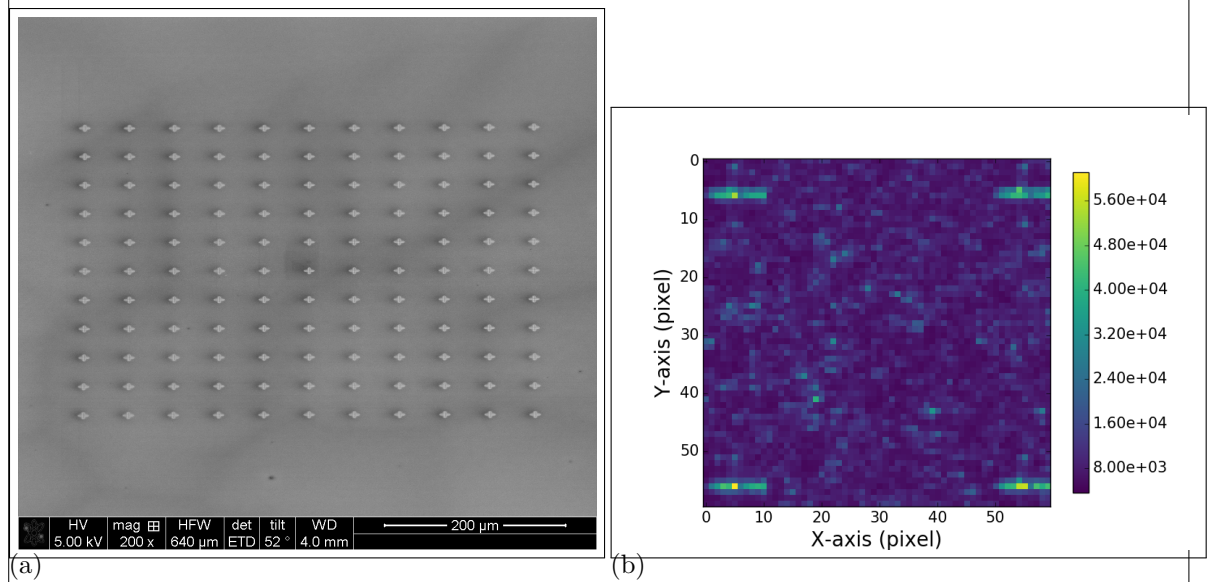


Figure 1.2: (a) Overview of a field of cross markers. The field spans $0.5 \times 0.5 \text{ mm}$ (b) White light scan of an area with a cross marker in all four corners.

1.1.2 Determination of The Position of Nanodiamonds

An nanodiamond pre-characterized in the confocal setup exhibiting the preferred spectroscopic properties has to be found again in the SEM setup where the nanomanipulator is installed. Therefore, we milled cross markers into the iridium coating of the silicon substrate using the focussed ion beam prior to spin-coating the substrate with nanodiamond solution. The crosses' size is $10 \times 10 \mu\text{m}^2$ are exhibit a nominal depth of 40 nm. Four crosses are the cornerpoints of a $50 \times 50 \mu\text{m}^2$ square. The 10×10 crosses spaned one field of crosses; we usually put 3 fields of crosses on one substrate.

To record the position of a nanodiamond with respect to a cross marker, we used two different methods:

- Scanning the sample in the confocal setup while a white light source illuminates the sample from the side in an acute angle. The edges of the cross markers are visible in the fluorescence scan. After turning the white light lamp off, the same area is scanned once more to record the fluorescence from the SiV centers. An overlay of the two images identifies the position of fluorescent SiV centers with respect to the cross markers. The disadvantage of this method is, that it takes a lot of time, as every scan has to be performed twice. Also, as only fluorescence light scans are performed, no information of the nanodiamonds is accessible. Such information comprises of the size of the individual nanodiamonds and whether the nanodiamonds lie isolated on the substrate surface. These parameters are only available during the pick-and-place process in the SEM. An emitter with optimal optical properties can turn out not to be suited for pick-and-place just before the process itself, hence the time spent to optically characterize an emitter was in vain.
- A more efficient method is scanning the substrate first in a commercial laser scanning microscope . The laser scanning microscope is a confocal microscope where the focus of a laser is used to obtain the height of a structure. It is possible to scan a whole field of cross markers in several minutes. The obtained image is a greyscale image, where the greyscale corresponds to the height deviation of a structure. Therefore, both the crosses and the nanodiamonds appear in darker shades of grey. So in contrast to the previous method, information on the size and isolation of the nanodiamonds is accessible. After scanning the substrate with the laser scanning microscope, it is put into the confocal setup. While observing the surface with the CCD camera (Figure 1.16), a specific cross marker is chosen as the starting point of a fluorescence light scan. Comparing the laser scanning microscope image and a fluorescence light scan, fluorescent dots of the fluorescence light scan are attributed to nanodiamonds in the laser scanning microscope scan (see Figures 1.11a and 1.11b).

fib pa-
rameter

put in
a pic of
white-
lightscan

specs

verify
info

1.1.3 The Pick-And-Place Process

After we identified nanodiamonds as well-suited for transfer to the target structure, both the substrate with the nanodiamonds and the target structure were mounted inside the SEM. The process was performed using a high resolution mode with a low acceleration voltage of the SEM of 1 keV and a current of 1.7 nA. The tip is approached to the pre-selected nanodiamond from above. As the SEM objective is mounted above the nanomanipulator, the proximity the nanomanipulator tip to the nanodiamond is not observable. The proximity is

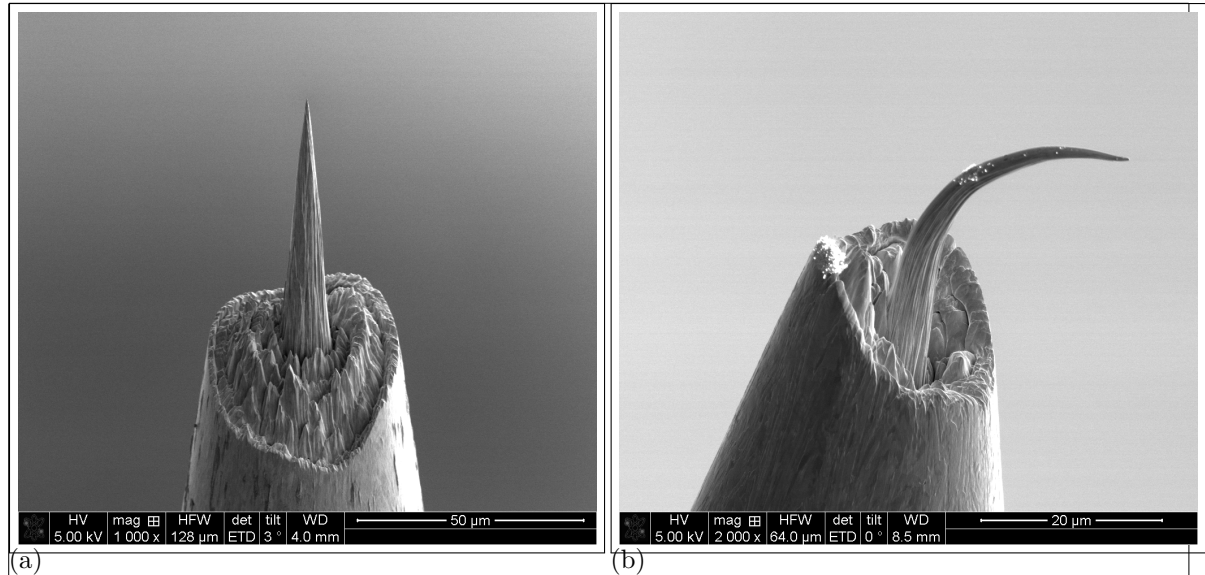


Figure 1.3

indirectly estimated by the shadow the tip casts onto the substrate and the focus. The first method is used for the coarse approachment of the tip to the nanodiamond: The closer the tip gets to the nanodiamond, the closer the shadow of the tip coincides with the nanodiamond position. Exploiting the focus as an estimate for the proximity of the tip is used for fine adjustment during the last stage of the approachment. This is done as follows: At the end of the coarse movement, the tip of the nanomanipulator is still some distance above the nanodiamond. The SEM is focused on the nanodiamond, therefore the nanomanipulator tip is out of focus and appears blurry. As the tip is approached, it moves further and further into focus, its image becoming sharper, until the it touches the nanodiamond. As this is a tricky process, sometimes the tip was approached with too much force and was destroyed in the process (Figure 1.3b).

When performed correctly, due to adhesion, the nanodiamond sticks to the nanomanipulator tip when the both get in contact (Figure 1.14a). The nanomanipulator is then moved to the target structure and the same approachment procedure is applied. Dependent on the material of the target structure, the nanodiamond either sticks to the structure right away due to higher adhesion forces between the nanodiamond and the structure (as is the case for the golden plasmonic antennas). Or the nanodiamond has to be "wiped off" of the nanomanipulator tip in a sideways motion. In either way it is possible to place the nanodiamond within a precision of a few nanometers.

1.2 Coupling SiV centers to Vertical-Cavity Surface Emitting Lasers

For metrology, the photon flux rate has to be high enough to be measured by a low optical flux detector [1].

The red AlGaInP-based oxide-confined vertical-cavity surface emitting lasers (VCSEL) are

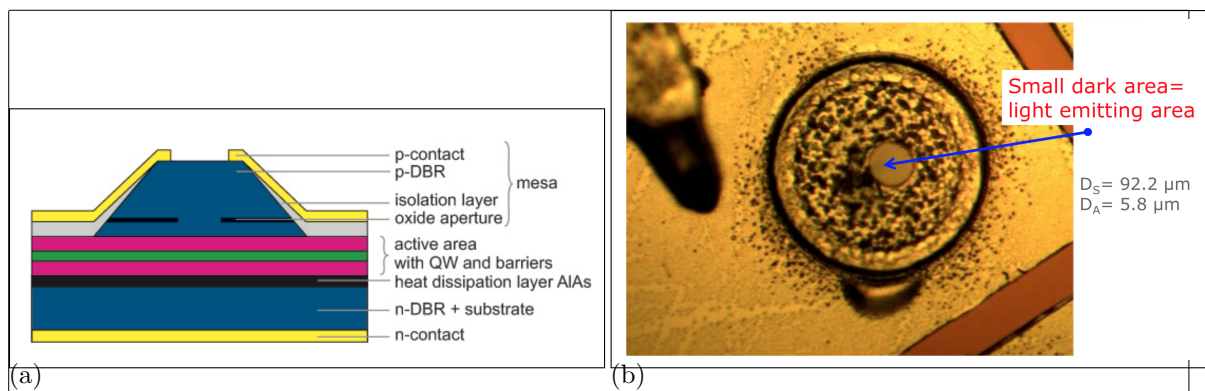


Figure 1.4: (a) Sketch of the VCSEL showing the different layers.

ask how to cite

(b) Image of the VCSEL. The circle with the black dots is the hole in the p-contact (diameter D_S , the smaller darker area in the middle is the laser output area (diameter D_A)

compact and perfect candidates for excitation of SiV centers in a hybrid integrated single photon source: They exhibit wavelengths around 650 nm at continuous wave emission. SiV centers exhibit intensity maxima at an excitation at 670 nm and 690 nm [1]. In addition, VCSELs exhibit circular beam profile, have low divergence angle and emit linearly polarized light.

diagram
einfuegen

1.2.1 Vertical-Cavity Surface Emitting Laser Structure

The VCSEL structure (??) consists of an active region between two distributed Bragg reflectors (DBR). The bottom n-type DBR is made of 50 pairs of AlAs/Al_{0.5}Ga_{0.5}As, the p-type DBR consists of 36 Al_{0.95}Ga_{0.05}As/Al_{0.5}Ga_{0.5}As mirror pairs [2]. The active region consists of four GaInP quantum wells (QW). An oxide aperture in a field node of the standing wave serves as a spatial filter for maximum modal gain by confining the current and the optical mode. The active diameter which is defined by the oxide aperture amounts to 5.8 μm. As this region is the area where the laser emission exits the VCSEL, the nanodiamonds have to be put within this area. The used VCSEL exhibits an optical output power up to 1 mW with low threshold current of up to 3 mA at about 655 nm.

ist das
up to

nachdenke
wie for-
mulierung
richtig
ist

was it
single?

1.2.2 SiV center in a Vertical-Cavity Surface Emitting Laser

As diamond material we used CVD grown nanodiamonds. They had been grown on an iridium coated silicon wafer (see ??). These nanodiamonds exhibit a nominal size of 200 nm. First, we selected a nanodiamond which exhibited one dominant line at 746.0 nm with a linewidth of 1.9 nm. Consecutively, its position on the substrate was determined using a white light laser scan as described in ?? . It was then transferred to the VCSEL Bm4 described in ?? . After a successful transfer of the pre-selected nanodiamond onto the active area of VCSEL Bm4, the VCSEL was put in the confocal setup. Using the laser from the confocal setup we checked if the pick-and-place process caused any modification of the spectroscopic properties of the SiV center such as a decrease of countrate or a modification of the fluorescence light spectrum. For this, the VCSEL itself was not operated itself. First, the VCSEL surface was

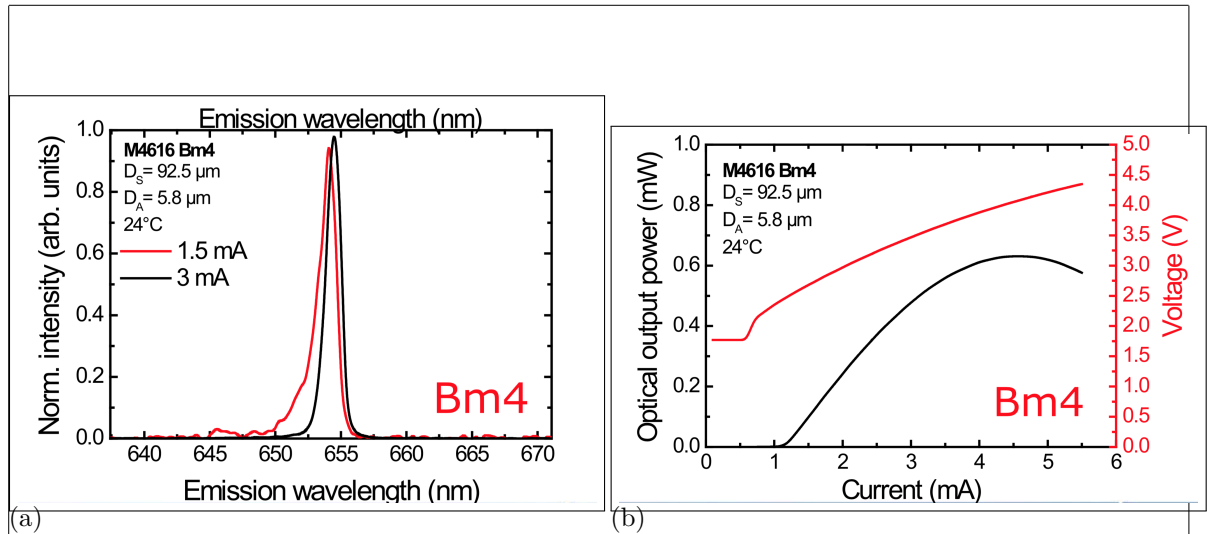


Figure 1.5: (a) Emission spectrum of the used VCSEL at two different currents. (b) Optical output power and voltage of the same VCSEL in dependence of input current. []

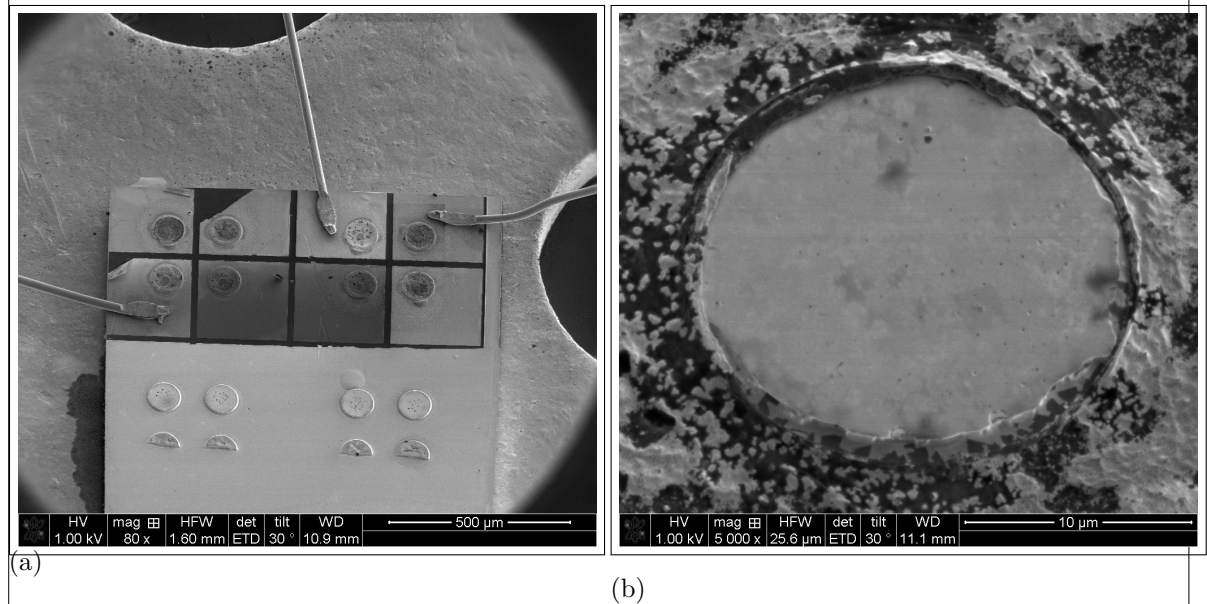


Figure 1.6: (a) SEM image of an array of VCSELs. The three wires are the anodes, which are connected to the top layer (p-contact) of the VCSEL. Therefore, three of the VCSEL structures can be operated. (b) Detail SEM image of the top of the exploited VCSEL Bm4. The circular middle part is the hole in the p-contact through which the top DBR is visible. The active diameter is smaller than that and not visible in the SEM.

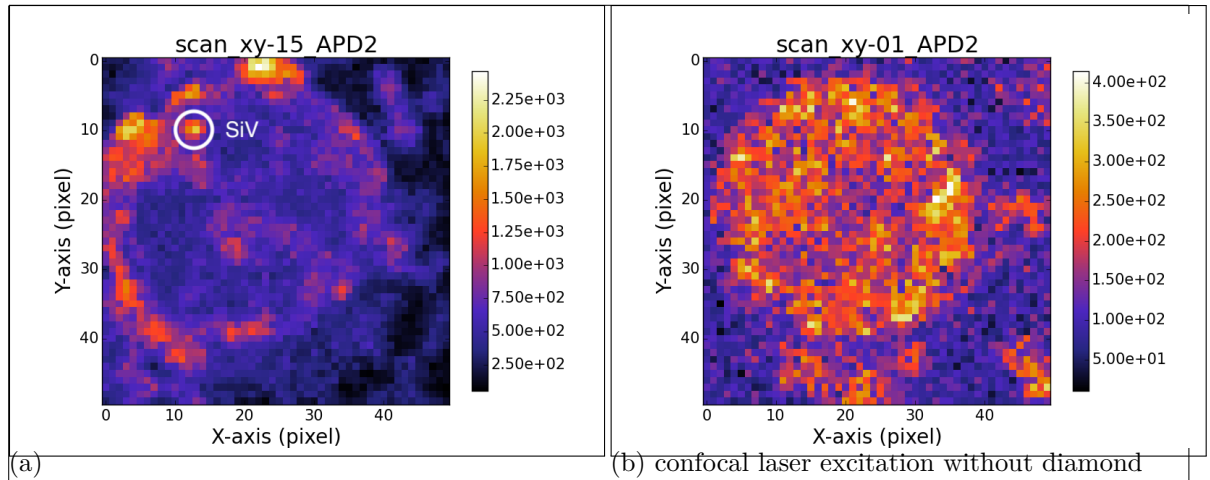


Figure 1.7: (a) Scan of the VCSEL Bm4 with coupled nanodiamond under excitation with the laser from the confocal setup. The big visible ring is the edge of the circular hole in the p-contact. The bright spot in the upper left corner corresponds to the transferred nanodiamond containing an SiV center. (b) Scan of the VCSEL Bm2 without nanodiamond under excitation with the laser from the confocal setup. The circular hole in the p-contact exhibits a constant countrate.

scanned Figure 1.7a. . A bright dot exhibiting a countrate of a few thousand counts per second is visible where the nanodiamond containing an SiV was put. A comparative scan of a VCSEL without nanodiamond only exhibits a background countrate, as expected (Figure 1.7b).

The spectrum of the SiV center in the transferred nanodiamond was investigated before and after the pick-and-place process (Figure 1.9). The original spectrum before nanodiamond transfer exhibits a sharp line at 746.0 nm (denoted line A). After the pick-and-place process, this line is still there, albeit with a low intensity. Another line at 700 nm (denoted line B) which was a minor feature in the spectrum before pick-and-place, is the predominant line after the process. This modification of the spectrum is caused by a reduction of the intensity of line A and constant intensity of line B. The reduction of the intensity of line A may be caused by damage of the color center due to electron radiation. While the energy of the electrons is low compared to the ionization energy of the color center , we observed a reduction of fluorescence light intensity after electron radiation .

check
number

numbers

put alex
meyers
observations
in appendix

besser
begruen-
den, was
passiert

1.3 Coupling Nanodiamonds to Double Bowtie Antenna Structures

1.3.1 Nanodiamond With Multiple SiV centers Coupled to Antenna

1.3.2 Nanodiamond With Single SiV center Coupled to Antenna

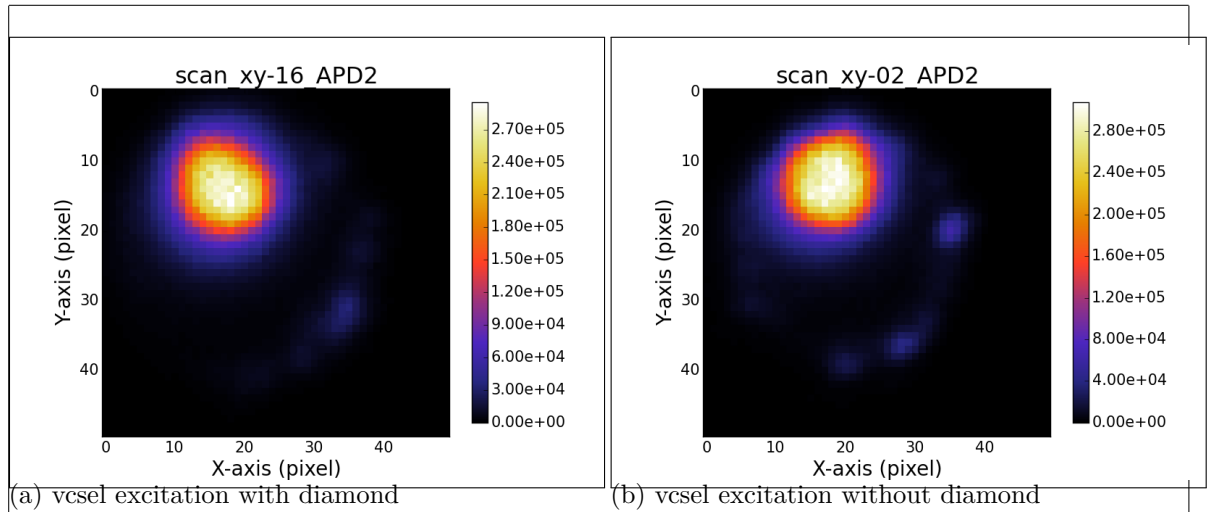


Figure 1.8: (a) longpass filter 720 (b) longpass filter 710

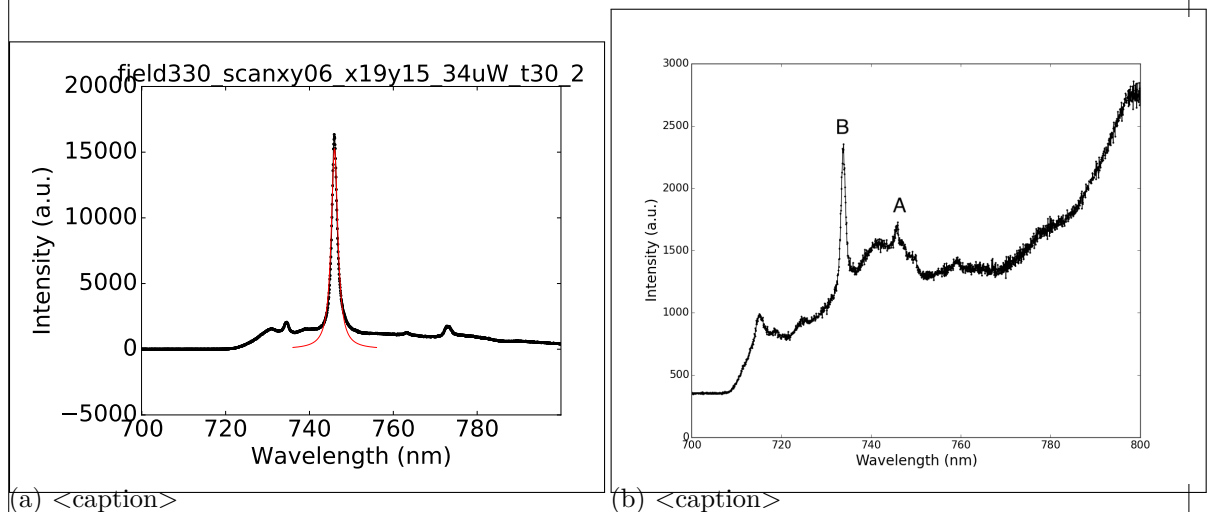


Figure 1.9: <caption>

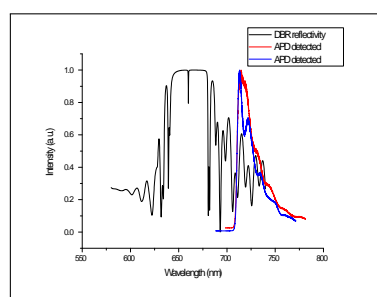
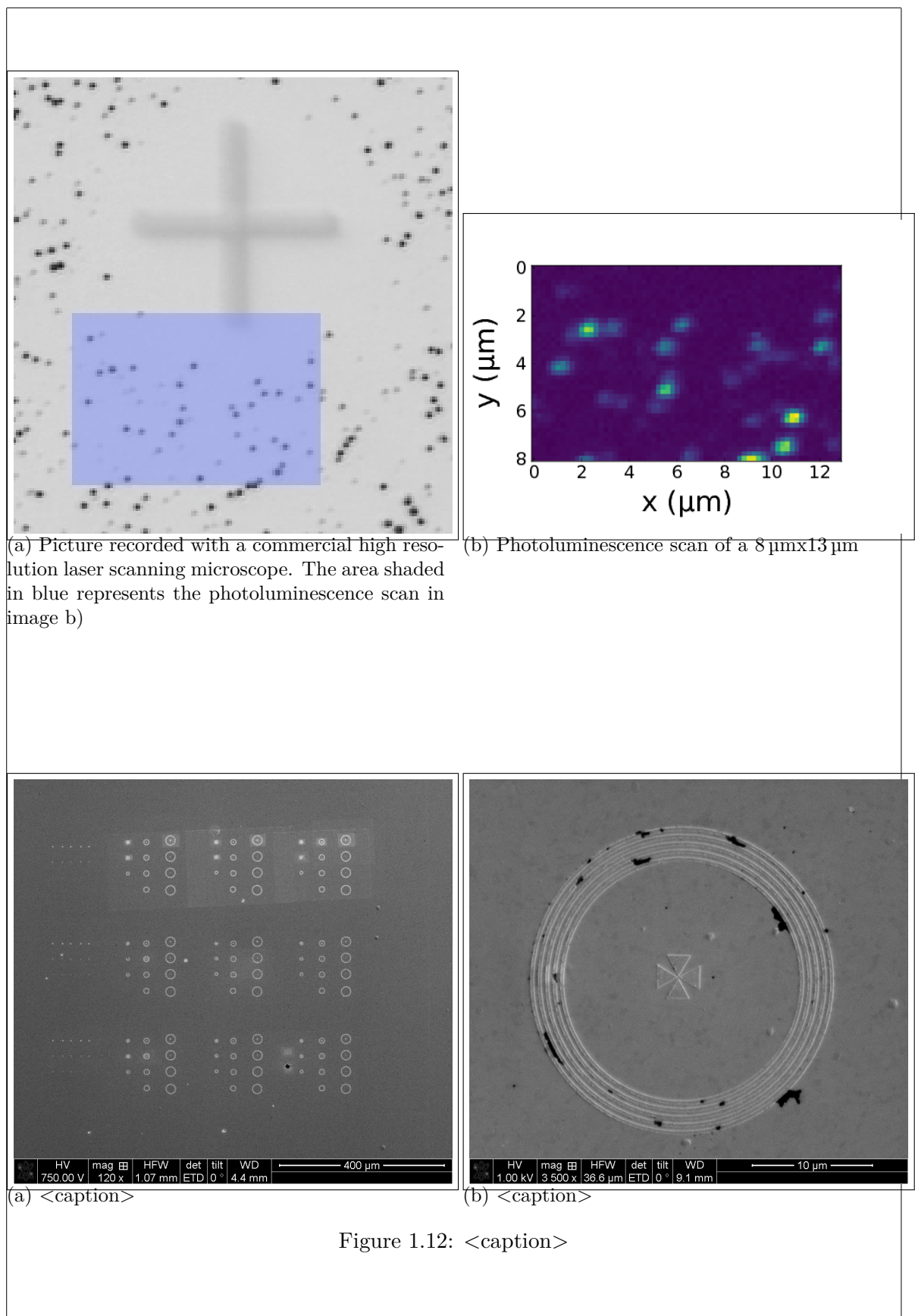


Figure 1.10: Reflectivity of the DBR of the VCSEL, and spectra of the VCSEL measured in the confocal setup.



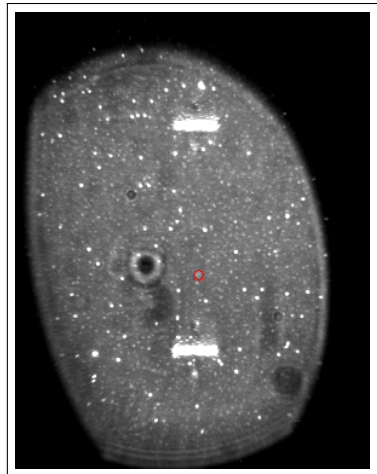


Figure 1.13: <caption>

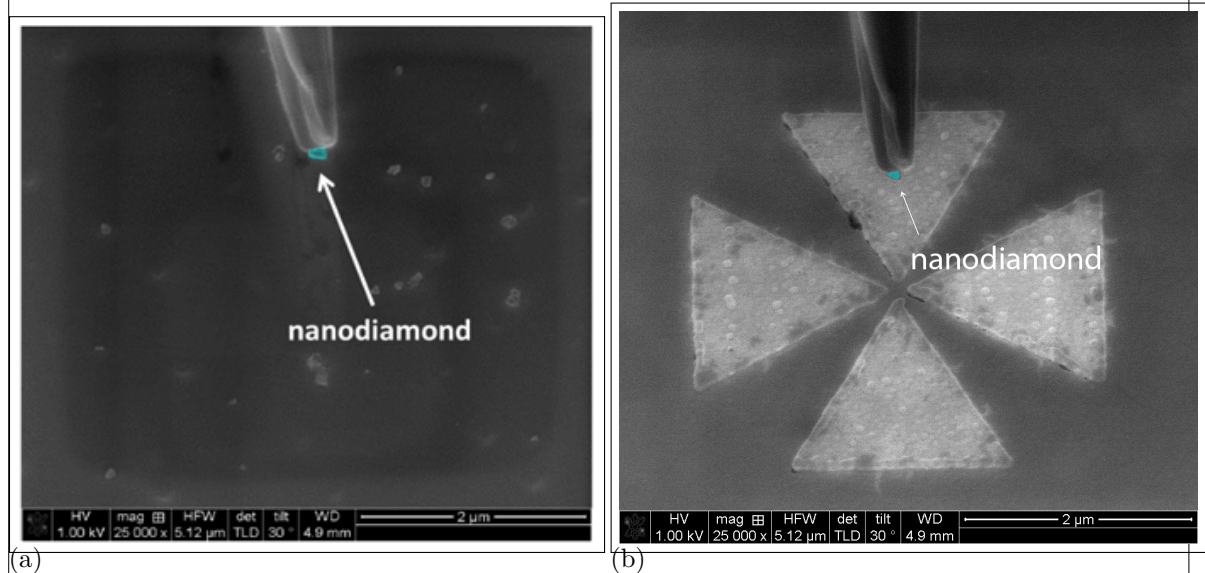


Figure 1.14

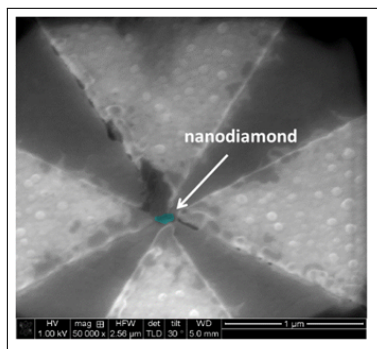


Figure 1.15: <caption>

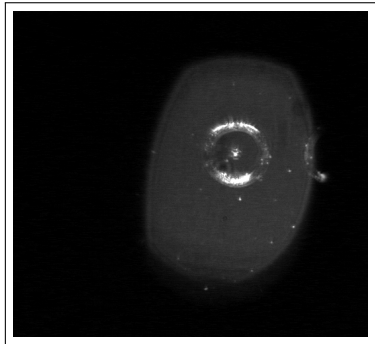


Figure 1.16: <caption>

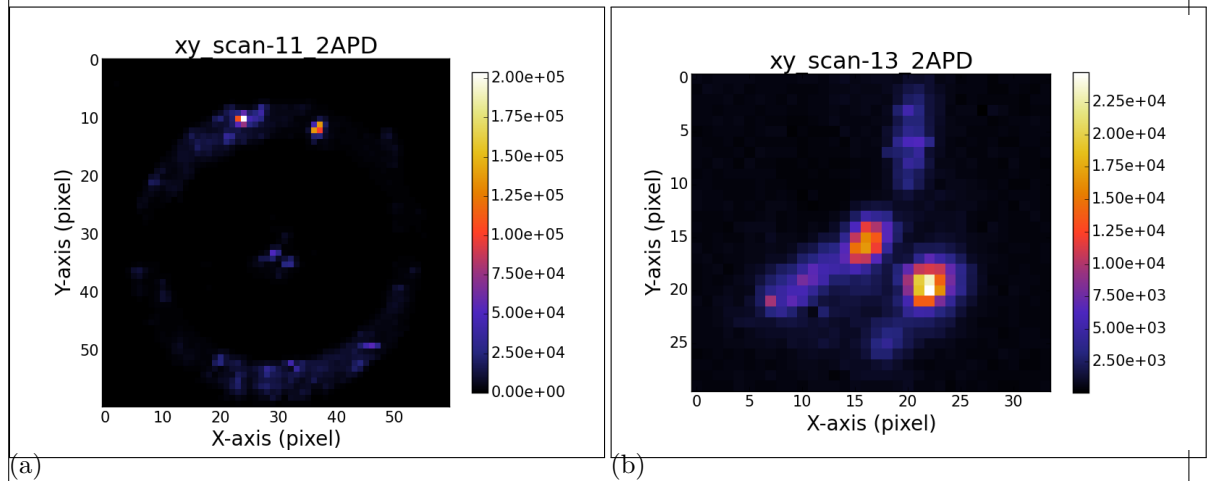


Figure 1.17: <caption>

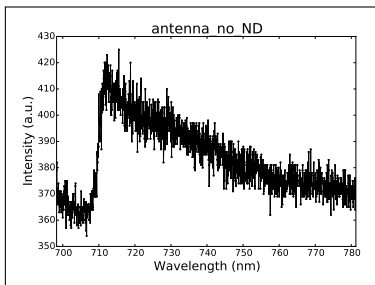


Figure 1.18: <caption>

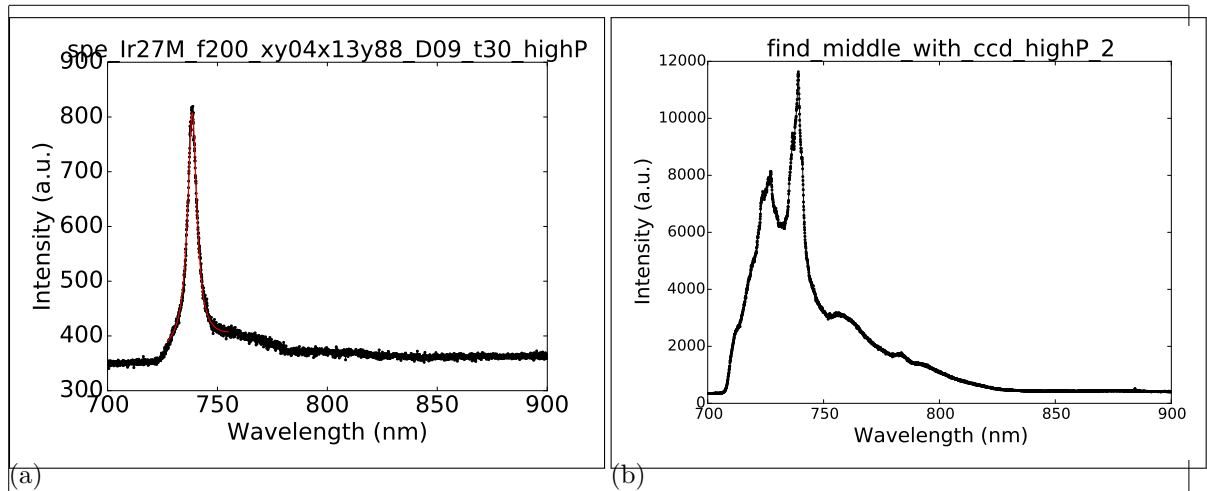


Figure 1.19: <caption>

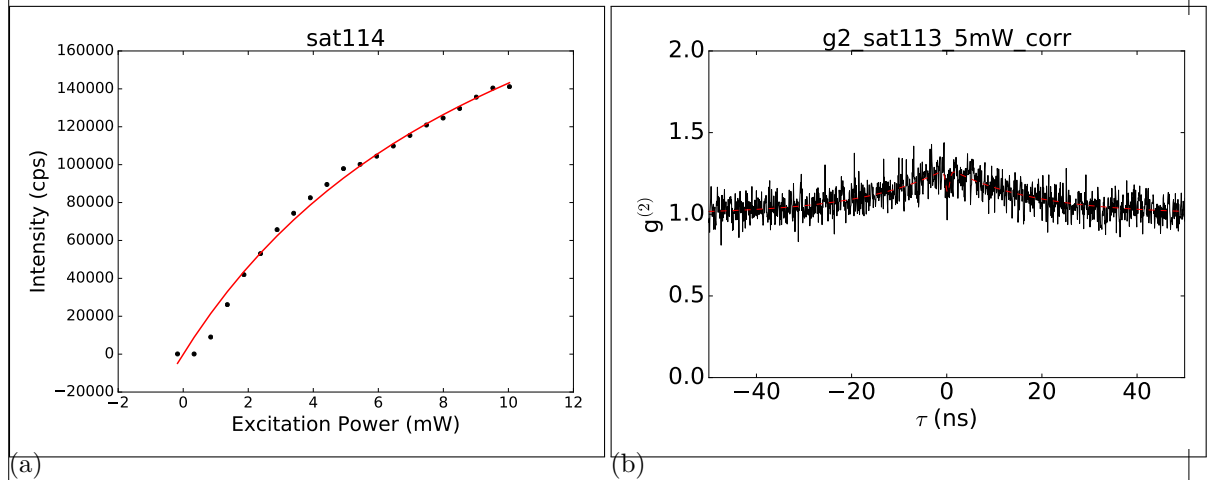


Figure 1.20: <caption>

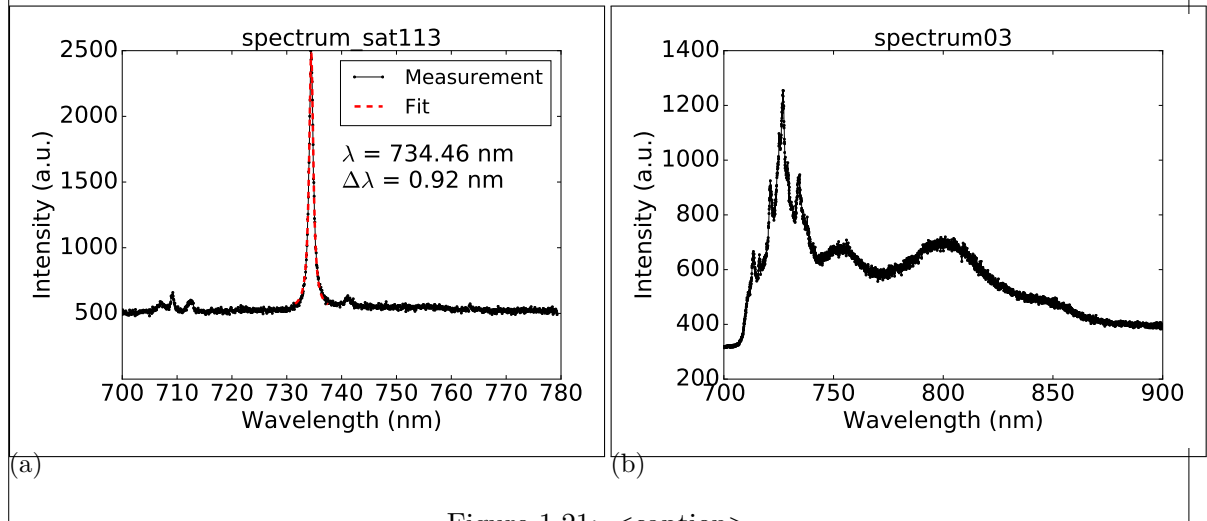


Figure 1.21: <caption>

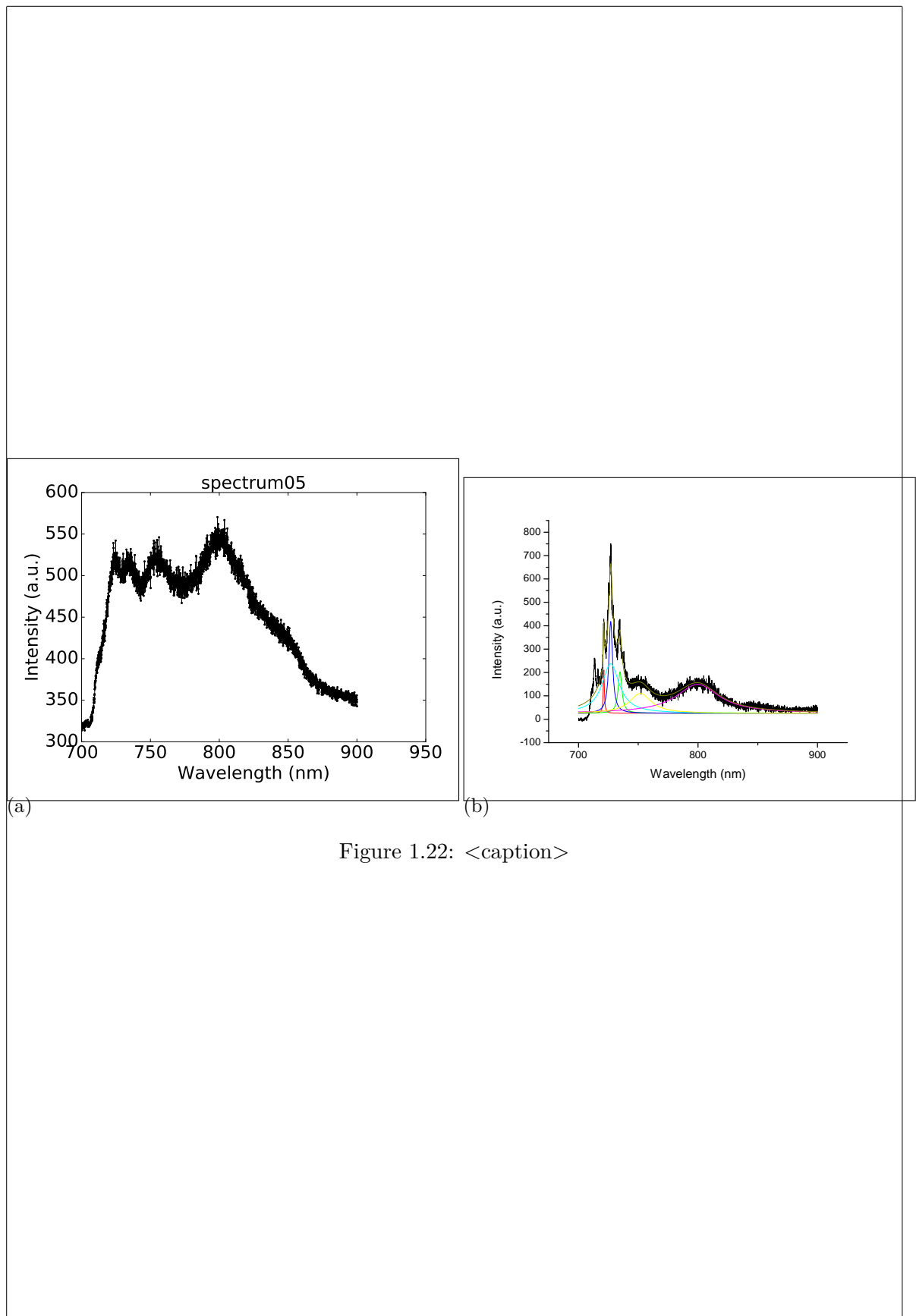


Figure 1.22: <caption>

Bibliography

- [1] Aigar Vaigu, Geiland Porrovecchio, Xiao Liu Chu, Sarah Lindner, Marek Smid, Albert Manninen, Christoph Becher, Vahid Sandoghdar, Stephan Götzinger, and Erkki Ikonen. Experimental demonstration of a predictable single photon source with variable photon flux. *Metrologia*, 54(2):218–223, 2017. 1, 5
- [2] Susanne Weidenfeld, Hendrik Niederbracht, Marcus Eichfelder, Michael Jetter, and Peter Michler. Transverse mode and polarization characteristics of AlGaInP-based VCSELs with integrated multiple oxide apertures. In Krassimir Panajotov, Marc Sciamanna, Angel Valle, and Rainer Michalzik, editors, *Proc. SPIE*, volume 8432, page 843205, jun 2012. 6